NASA Technical Memorandum 102536

Evaluation of Thermal and Mechanical Loading Effects on the Structural Behavior of a SiC/Titanium Composite

Joseph E. Grady and Bradley A. Lerch
Lewis Research Center
Cleveland, Ohio

Prepared for the
31st Structures, Structural Dynamics and Materials Conference
cosponsored by the AIAA, ASME, ASCE, AHS, and ASC
Long Beach, California, April 2-4, 1990

NASA

EVALUATION OF THERMAL AND MECHANICAL LOADING EFFECTS ON THE STRUCTURAL BEHAVIOR OF A SiC/TITANIUM COMPOSITE

Joseph E. Grady and Bradley A. Lerch
National Aeronautics and Space Administration
Lewis Research Center
Cleveland, Ohio 44135

E-5349

SUMMARY

Composite specimens of titanium-15-3 matrix reinforced with continuous SCS-6 silicon carbide fibers were tested under a variety of thermal and mechanical loadings. A combined experimental/finite element approach was used to estimate the effective in-situ modulus of the matrix material and to evaluate changes in modulus due to the applied loads. Several fiber orientations were tested. Results indicate that the effect of the thermal loads on composite stiffness varies with fiber orientation. Applications of this method to test specimens damaged by uniaxial tension, thermal cycling, and isothermal fatigue loadings are used to illustrate that by monitoring overall structural behavior, changes in stiffness caused by thermomechanical loading can be detected.

INTRODUCTION

The mechanical behavior of composite materials depends on the properties of the fiber and matrix constituents. Because of inhomogeneities due to the addition of the fibers and due to thermal loadings which occur during the fabrication process, the in-situ matrix properties of the SiC/Ti-15-3 composite can vary significantly from those of the monolithic matrix (ref. 1). Matrix stiffness properties, as well as the integrity of the fiber/matrix bond, will also change as the composite material deforms under applied mechanical and thermal loads.

In this paper, an indirect measurement of the effective in-situ matrix modulus is obtained, using the results of experimental tests together with finite element analysis of the composite test specimens. The term "effective matrix modulus" is used to account for changes in the measured stiffness of the composite. These changes could be due to a variety of damage modes. In this article, however, all damage will be incorporated into and accounted for by changes in matrix modulus. The resonant frequencies of the individual specimens are measured by vibration testing. Based on the measured frequencies, the effective modulus of the test specimens is determined by finite element analysis. This indirect measurement technique is applied to each individual test specimen in its original, as-fabricated condition, as well as after a heat treatment, and thermal or mechanical loads are applied. The results therefore show how the effective matrix modulus changes with the different applied loads.

EXPERIMENTAL PROCEDURE

Material Fabrication

The composite was fabricated in a proprietary process in which alternating layers of SiC (SCS-6) fibers and foils of Ti-15V-3Cr-3Sn-3Al (Ti-15-3) were consolidated. Eight rows of fibers were used, yielding a total composite thickness of approximately 0.08 in. The nominal fiber volume fraction was 34 percent. Additional microstructural details of the material can be found in references 2 and 3. Several fiber orientations were used in this study, consisting of a $[90]_8$, $[\pm30]_{2S}$, $[\pm45]_{2S}$, $[0/90]_{2S}$, and $[90/0]_{2S}$. The [0/90] had 0° plies on the outer surfaces, whereas the [90/0] had 90° plies on the outer surfaces. Test specimens, as shown in figure 1(a), of nominal dimension 6 by 0.5 by 0.08 in. and containing a reduced gauge section were cut from the finished panels.

Vibration Testing

Test specimens were cantilevered in mechanical grips that clamped 2 in. along one end of the specimen, as shown in figure 2, A lightweight (142 mg) accelerometer was attached to the mid-span of the specimen using a thin layer of MIL-A-46050C cyanoacrylate adhesive. Free vibration response of the cantilevered specimen was recorded digitally on a spectrum analyzer, and simultaneously displayed on an oscilloscope, as shown in figure 3. Figures 3 and 4 show representative measurements of the vibration response for a typical specimen. Figure 3 shows, as displayed on the oscilloscope, the acceleration response in the time domain to a transient load applied at the free end of the specimen. The corresponding frequency response is shown in figure 4. The frequency data was processed using a Hanning window for improved frequency resolution, and was obtained by RMS averaging the results of ten separate tests for each specimen. After the signal averaging was performed, resonant frequencies were identified by digitally locating the peaks in the frequency response signal. Measurements taken in this manner proved to be both extremely sensitive to material changes (e.g., cracking, debonding) caused by the applied loads, and repeatable to within a ±0.2 percent measurement error.

ANALYSIS

Material Properties

Stiffness coefficients for the 8-ply composite test specimens were calculated from the fiber and matrix properties given in table I as follows. For a single unidirectional ply with fibers oriented in the 1-direction, the elastic constants given by simple rule-of-mixtures calculations are (ref. 4):

$$E_{11} = V_f E_f + V_m E_m$$

$$\nu_{12} = V_f \nu_f + V_m \nu_m$$

$$E_{22} = [V_f/E_f + V_m/E_m]^{-1} \qquad (1)$$

$$G_{12} = [V_f/G_f + V_m/G_m]^{-1}$$

$$\rho = V_f \rho_f + V_m \rho_m$$

where the subscripts f and m refer to fiber and matrix, E, G, ν, and ρ are the Young's Modulus, Shear Modulus, Poisson's ratio and mass density, respectively, and V is the volume fraction of the respective constituent.

Assuming a state of plane stress in the 1-2 plane, the unidirectional ply stress-strain relations are given by:

$$\begin{Bmatrix} \sigma_1 \\ \sigma_2 \\ \sigma_6 \end{Bmatrix} = [Q] \begin{Bmatrix} \varepsilon_1 \\ \varepsilon_2 \\ \varepsilon_6 \end{Bmatrix} \qquad (2)$$

where the subscripts 1, 2 denote normal in-plane stresses and strains; and 6 denotes in-plane shear. In terms of the engineering constants,

$$[Q] = [S]^{-1}$$

where

$$S_{11} = 1/E_{11} \qquad S_{12} = -\nu_{12}/E_{11}$$

$$S_{22} = 1/E_{22} \qquad S_{13} = S_{23} = 0 \qquad (3)$$

$$S_{66} = 1/G_{12}$$

Stress and strain transformation equations are used to calculate [Q] in equation (2) for unidirectional ply oriented at an arbitrary angle θ to the 1- direction, and laminated plate theory (ref. 5) is then used to calculate membrane and bending stiffness coefficients for the 8-ply composite with arbitrarily oriented plies. These coefficients are then used as the elastic anisotropic constants in the finite element analysis.

The simplifying assumptions inherent in equation (1) are that the fiber/matrix bond is strong and the deformation is elastic. The latter assumption may be adequate in this case since the modulus calculations are being used to predict composite stiffness for small amplitude vibrations. The actual strength of the fiber/matrix bond in unknown.

Finite Element Analysis

A finite element modal analysis was performed for each test specimen using MSC/NASTRAN (ref. 6). Two-dimensional, isoparametric shell elements with orthotropic membrane and bending stiffness were used to model the composites. A representative finite element mesh used to analyze the cantilevered tensile specimen with a reduced gage section is shown in figure 1(b).

RESULTS AND DISCUSSION

Numerical Convergence

A preliminary study was performed to determine the number of finite elements required for a converged modal solution. The results shown in figures 5 (a) and (b) are the natural frequencies measured and calculated for a $[\pm 30]_{2S}$ specimen of dimension 6 by 1 by 0.075 in. These figures indicate that the calculated bending frequencies are sensitive to the number of elements in the longitudinal direction. A converged solution is obtained with 30 longitudinal elements, and these results are given in table II. Bending stiffness is underestimated with coarser meshes because reduced integration is used to calculate the element stiffness (ref. 6). Thus, 30 longitudinal elements were used in subsequent calculations.

Vibration Analysis

Vibration tests were performed several times for a few, selected specimens to determine the measurement repeatability. The measured values for natural frequencies were found to vary a maximum of 0.2 percent from one test to another. Shifts in frequency due to applied thermal and mechanical loads were usually on the order of 2 to 3 percent, so this degree of measurement accuracy was considered acceptable.

The placement of the accelerometer on the specimen, as shown in figure 2, was chosen so as to detect the flexural (bending) motion of the specimen rather than the torsional (twisting) motion. Therefore, in the results presented here, the frequencies are all associated with bending modes. The lowest frequency range scanned for the specimen used in figure 5 was 1 to 1.2 kHz, so no data was taken for the 180 Hz bending mode. The dashed lines are the measured resonant frequencies for each of the modes. The calculated frequencies were determined by varying the matrix modulus from 9 to 15 Msi until the frequencies calculated in the finite element analysis were within 1 to 2 percent of the measured values. The matrix modulus giving the best agreement with the measured values for this specimen was 10.3 Msi. The results in figures 5(a) and (b) and table II indicate that the frequencies calculated for the first six bending modes correspond well with the measured values.

Heat Treating

In figure 6, the effective matrix modulus is presented graphically for each of the ply orientations tested. The average matrix modulus, both before and after heat treating for 24 hr at 1292 °F in vacuum, is 10.7 Msi. This is

somewhat lower than the normal modulus of 12.5 Msi determined from a tensile test for monolithic Ti-15-3 (ref. 3). The two methods may yield different values. This is currently under investigation. Further, a perfect bond between fiber and matrix has been assumed in the stiffness calculations given in equation (1). Any imperfections in the fiber/matrix bond will lower the composite stiffness, and therefore appear as a lower matrix modulus in this model. Similarly fabrication-induced residual stresses can lead to cracking in the matrix or fiber/matrix interphase region. Both types of damage will lower the effective matrix modulus in these calculations. Nevertheless, the modulus values given here can be used effectively to compare the relative damage states of the different test specimens. The data in figure 6 are given in tables III to VII.

If $\Delta\Theta$ is the difference in ply orientation for neighboring plies of the composite, i.e.

$$\Delta\Theta = \Theta_i - \Theta_{i+1}$$

where the subscript ,i, refers to the ply number, the data in figure 6 indicate that heat treatment effectively increased the composite stiffness when $\Delta\Theta = 60°$ or less (i.e. [±30] or [90] fiber orientations), and decreased composite stiffness when $\Delta\Theta = 90°$ (i.e. [±45], [0/90] and [90/0] fiber orientations). These limited data suggest that the response of the composite to heat treatment is dependent on the residual stress state and on the lateral constraining effect that the plies impose on one another.

Tensile tests on monolithic Ti-15-3 (ref. 3) indicate that although tensile strength and failure strain are affected by the heat treatment, the elastic modulus is not significantly changed from its original value of approximately 12.5 Msi. The changes in effective matrix modulus of the composite caused by heat treating, therefore, are most likely due to changes in the integrity of the fiber/matrix bond that could occur during thermal loading of the composite. The integrity of this bond could be affected by the residual stress state within the individual plies and would therefore vary as a function of the ply stacking sequence. A detailed analysis of the residual stress state is in progress and will be reported subsequently.

Tensile Load

A 144 ksi tensile load was applied to a [±30] specimen after it was heat treated. The test was performed in strain control, and at a constant strain rate of 10^{-4} sec^{-1}. The maximum strain level reached was 1.5 percent, which is very close to the failure strain for this fiber orientation. An additional vibration test was performed on the specimen after the tensile load was removed. Effective matrix modulus values were back-calculated, based on the data given in table III are shown in figure 7. The matrix modulus was 11.6 Msi after heat treating but dropped to 10.3 Msi after applying the tensile load, suggesting that some damage to the composite was caused by the tensile load. Micro-focus x-ray analysis was performed on the damaged specimen. This analysis indicated that damage in the form of cracks was concentrated in the area highlighted in figure 8. Examination of the damaged area using a Scanning Electron Microscope (SEM) revealed the failure details shown in figure 8. As indicated in these micrographs, the outer matrix layer exhibits cracking. The

cracking occurs on both sides of the specimen in the area indicated by the dashed square. A high magnification of these cracks indicate that the fibers within the crack (i.e., the first fiber row) remain intact. Whether these cracks propagated through the thickness of the specimen is at this time unknown.

Fatigue Load

After heat treatment, a [±45] specimen was fatigue tested at a frequency of 0.1 Hz for 195 tension-tension cycles at 800 °F. The applied mean stress, σ_m, was 17.3 ksi and the stress range, $\Delta\sigma$, was 32.9 ksi. The stress ratio, $\sigma_{min}/\sigma_{max}$, was therefore 0.05. For these loading conditions, 195 cycles is approximately 1 percent of the expected low cycle fatigue life of the composite (ref. 7). The test data are given in table IV and the calculated modulus (10.7 Msi) is compared to the as-received (11.4 Msi) and heat treated (11.0 Msi) values in figure 9. The results indicate that some degradation was caused by the fatigue loading. No metallographic inspection of the damaged specimen has yet been performed, so no supporting data is available to identify the type and location of the damage. However, no visible cracking was observed on the outer surfaces of the specimen.

Thermal Cycling

Cyclic thermal loading may cause cracking at or near the fiber/matrix interface region due to the mismatch in thermal expansion coefficient between fiber and matrix. To evaluate this effect, the [90/0] specimen was exposed to 2000 thermal cycles from 200 to 1000 °F by cycling the specimen into and out of a furnace at a rate of 0.17 cycles/min. The test results are tabulated in table V and are shown graphically in figure 10. They indicate that the thermal cycling had a negligible effect on the composite stiffness. The difference between as-received and heat treated properties indicate that some damage may have been introduced during heat treatment, but the material was not significantly further damaged by the cyclic thermal load.

Further evidence to this effect was obtained by tensile testing several [0/90] specimens to failure. A typical specimen that had not been exposed to the thermal cycling had measured values of 22 Msi, 146 ksi and 1.04 percent for the modulus, E_{11}, ultimate tensile strength, and failure strain, respectively; while an otherwise identical specimen had corresponding values of 21 Msi, 137 ksi and 0.98 percent after being exposed to the cyclic thermal load. These results indicate that either no material degradation was caused by the thermal cycles, or that both the vibration analysis and tensile test were insufficient for detecting the small amount of damage which may have occurred during thermal cycling.

SUMMARY OF RESULTS

A combined experimental/analytical technique that uses the results of vibration testing together with finite element analysis, was demonstrated and used to evaluate the degradation of mechanical properties of SiC/Ti-15-3 composites. The effects of heat treatment on specimens of varying ply orientation were analyzed, and representative results were presented that illustrate

the effects of monotonic tensile loading, fatigue loading, and thermal cycling on composite stiffness.

The results for the five different ply orientations considered, indicated that the effective in-situ modulus of the matrix material in the as-received condition was an average of 15 percent lower than the monolithic value. In addition, the effect of heat treatment on the composite stiffness varied with ply stacking sequence.

REFERENCES

1. Bahei-El-Din, Y.A. and Dvorak, G.J., "Plastic Deformation of a Laminated Plate with a Hole," Journal of Applied Mechanics, Vol. 47, No. 4, Dec. 1980, pp. 827-832.

2. Lerch, B.A., Hull, D.R., and Leonhardt, T.A., "As-Received Microstructure of a SiC/Ti-15-3 Composite," NASA TM-100938, 1988.

3. Lerch, B.A., Gabb, T.P., and MacKay, R.A., "Heat Treatment Study of the SiC/Ti-15-3 Composite System," NASA TP-2970, 1990.

4. Jones, R.M., Mechanics of Composite Materials, Scripta Book Co., Washington, DC, 1975.

5. Whitney, J.M., Structural Analysis of Laminated Anistropic Materials, Technomic Publishing Co., Lancaster, PA, 1987.

6. MacNeal, R.H., ed., The NASTRAN Theoretical Manual, (Level 15.5), MacNeal-Schwendler Corp., Los Angeles, CA, 1972.

7. Lerch, B.A., On-going research, NASA-Lewis Research Center, Cleveland, OH.

TABLE I. - FIBER AND MATRIX
ELASTIC PROPERTIES

	Fiber	Matrix
E,(Msi)	62	9-15
G,(Msi)	26	E/2(1+ν)
ν	0.19	0.32
ρ,(lb/in^3)	0.108	0.172
α,(x 10^{-6}/°F)	2.7	4.7

TABLE II. - SPECIMEN #25 $[\pm 30]_{2s}$
FREQUENCY DATA
[m - Measured value (Hz); c - calculated value (Hz).]

Vibration mode	As-received condition		
	ω_m	ω_c*	Percent error
1	------	181.9	---
2	1 131	1 136	0.4
3	3 190	3 188	0.1
4	6 212	6 274	1.0
5	10 270	10 410	1.4
6	15 300	15 585	1.9

*E_m = 10.3 Msi.

TABLE III. SPECIMEN #24 $[\pm 30]_{2s}$ FREQUENCY DATA
[m - Measured value (Hz); c - calculated value (Hz).]

Vibration mode	As-received condition			After heat treatment*			After tensile loading†		
	ω_m	ω_c‡	Percent error	ω_m	ω_c§	Percent error	ω_m	ω_c‖	Percent error
1	------	183.7	----	------	188.7	----	------	182.7	----
2	1 146	1 144	0.15	1 179	1 176	0.25	1 138	1 138	0.02
3	------	3 215	----	------	3 304	----	------	3 199	----
4	6 308	6 325	0.27	6 471	6 498	0.42	6 199	6 292	1.5
5	10 393	10 460	0.64	10 968	10 748	2.0	10 713	10 405	2.9
6	15 435	15 743	2.0	16 260	16 239	0.13	15 705	15 651	0.3

*1292 °F for 24 hr.

†144 ksi (1.5 percent strain).

‡E_m = 10.5 Msi.

§E_m = 11.6 Msi.

‖E_m = 10.3 Msi.

TABLE IV. - SPECIMEN #A1 $[\pm 45]_{2s}$ FREQUENCY DATA

[m - Measured value (Hz); c - calculated value (Hz).]

Vibration mode	As-received condition			After heat treatment*			After fatigue loading†		
	ω_m	ω_c‡	Percent error	ω_m	ω_c§	Percent error	ω_m	ω_c‖	Percent error
1	-----	129.3	-----	------	127.4	----	-----	126.1	----
2	958.3	958.6	0.03	945.5	945.1	0.04	934.5	935.0	0.05
3	2754	2807	1.9	2722	2768	1.7	2691	2739	1.8
4	5448	5479	0.57	5270	5403	2.5	5280	5346	1.3

*1292 °F for 24 hr.

†195 LCF Cycles at 800 °F.

‡E_m = 11.4 Msi.

§E_m = 11.0 Msi.

‖E_m = 10.7 Msi.

TABLE V. - SPECIMEN #C1 $[90/0]_{2s}$ FREQUENCY DATA.

[m - Measured value (Hz); c - calculated value (Hz).]

Vibration mode	As-received condition			After heat treatment*			After thermal cycling†		
	ω_m	ω_c‡	Percent error	ω_m	ω_c§	Percent error	ω_m	ω_c‖	Percent error
1	140.0	140.0	0.0	138.0	137.5	0.4	137.5	137.5	0.0
2	1015	1024	0.86	999.0	1006	0.7	1031	1006	2.4
3	2906	2980	2.5	2875	2928	1.8	2969	2928	1.4
4	5659	5798	2.5	5583	5697	2.0	5808	5697	1.9

*1292 °F for 24 hr.

†2000 cycles: 200 to 1000 °F.

‡E_m = 10.7 Msi.

§E_m = 10.1 Msi.

‖E_m = 10.1 Msi.

TABLE VI. - SPECIMEN #B7 $[0/90]_{2s}$ FREQUENCY DATA

[m - Measured value (Hz); c - calculated value (Hz).]

Vibration	As-received condition			After heat treatment*		
	ω_m	ω_c†	Percent error	ω_m	ω_c‡	Percent error
1	151.3	151.4	0.07	150.3	151.1	0.6
2	1102	1107	0.48	1093	1105	1.1
3	3161	3222	1.9	3125	3216	2.9
4	6130	6269	2.3	6081	6257	2.9

*1292 °F for 24 hr.

†E_m = 9.2 Msi.

‡E_m = 9.1 Msi.

TABLE VII. SPECIMEN #38 $[90]_8$ FREQUENCY DATA

[m - Measured value (Hz); c - calculated value (Hz).]

Vibration mode	As-received condition			After heat treatment*		
	ω_m	ω_c †	Percent error	ω_m	ω_c ‡	Percent error
1	180.5	180.6	0.1	182.0	182.1	0.04
2	-----	1319	---	------	1330	----
3	3740	3832	2.4	3800	3863	1.6
4	7210	7479	3.7	7328	7539	2.9

*1292 °F for 24 hr.

†E_m = 11.3 Msi.

‡E_m = 11.5 Msi.

TABLE VIII. - TEST SPECIMEN GEOMETRY

[Dimensions in inches, weight in grams.]

Test specimen designation	Fiber orientation	Specimen length	Gage length	Gage width	Thickness	Weight
A1	$[\pm 45]_{2s}$	5.980	1.5	0.317	0.076	13.012
B7	$[0/90]_{2s}$	5.984	1.5	.329	.077	13.374
C1	$[90/0]_{2s}$	5.990	1.5	.329	.077	13.440
24	$[\pm 30]_{2s}$	5.877	(*)	.999	.075	30.105
25	$[\pm 30]_{2s}$	5.872	(*)	.746	.075	22.283
38	$[90]_8$	5.510	1.0	.328	.083	13.765

*Rectangular specimen.

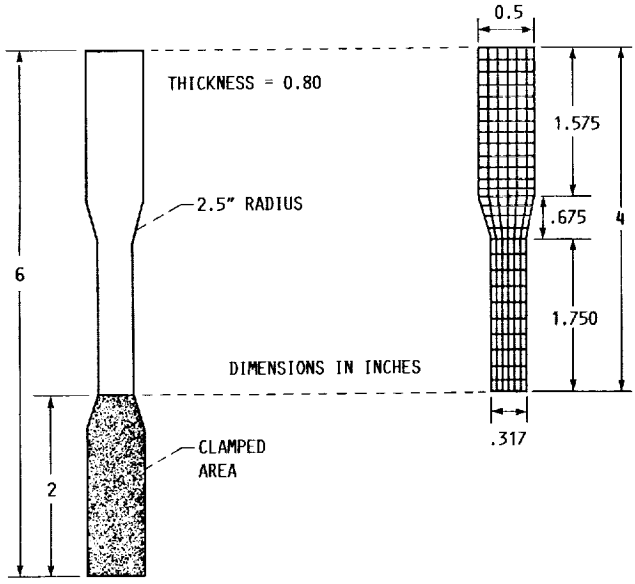

(a) TEST SPECIMEN. (b) FINITE ELEMENT MODEL.

FIGURE 1. - TEST SPECIMEN GEOMETRY.

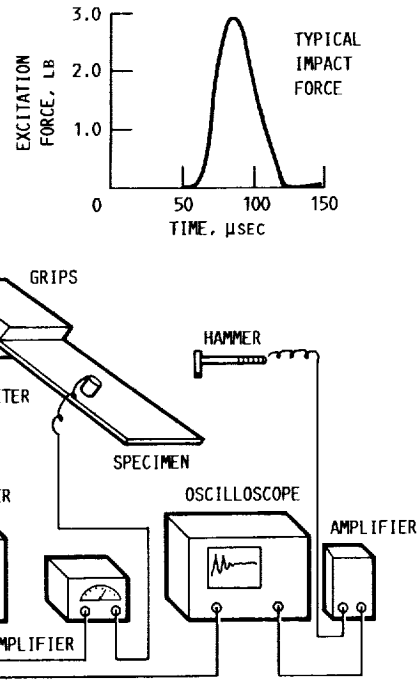

FIGURE 2. - EXPERIMENTAL APPARATUS.

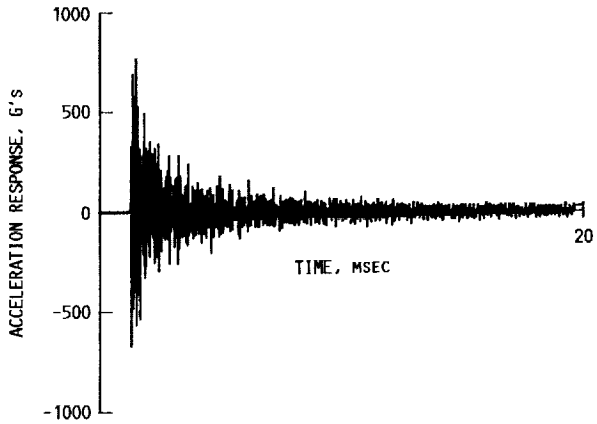

FIGURE 3. - ACCELEROMETER MEASUREMENT OF FREE VIBRATION RESPONSE OF SPECIMEN NO. 25 AFTER HEAT TREATMENT.

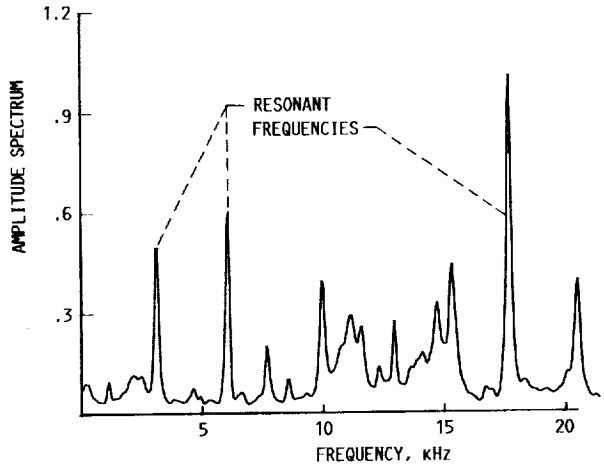

FIGURE 4. - AMPLITUDE SPECTRUM FOR SPECIMEN NO. 25 AFTER HEAT TREATMENT.

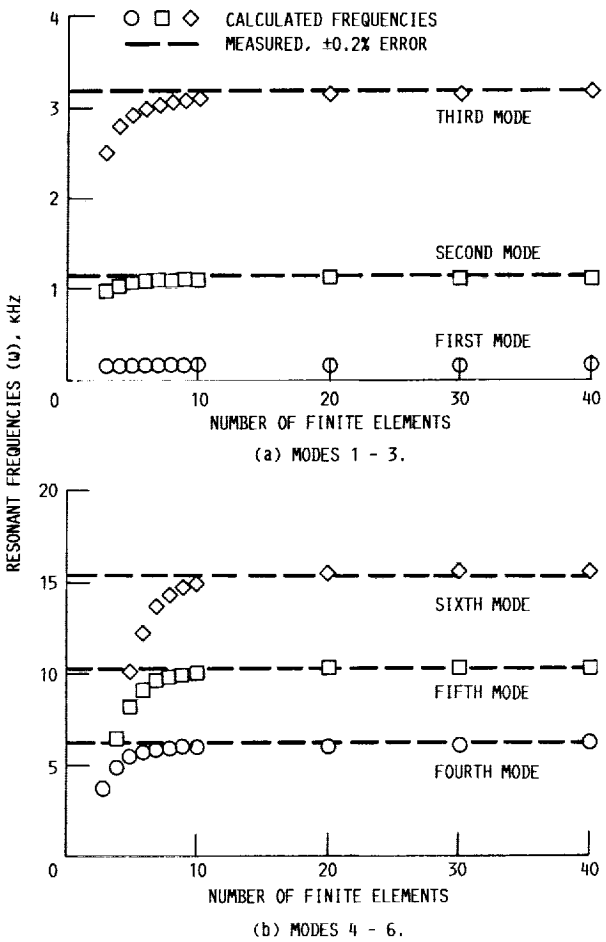

FIGURE 5. - FINITE ELEMENT MESH CONVERGENCE: TEST SPECIMEN NO. 25, [±30]; MATRIX MODULUS: 10.3 MSI.

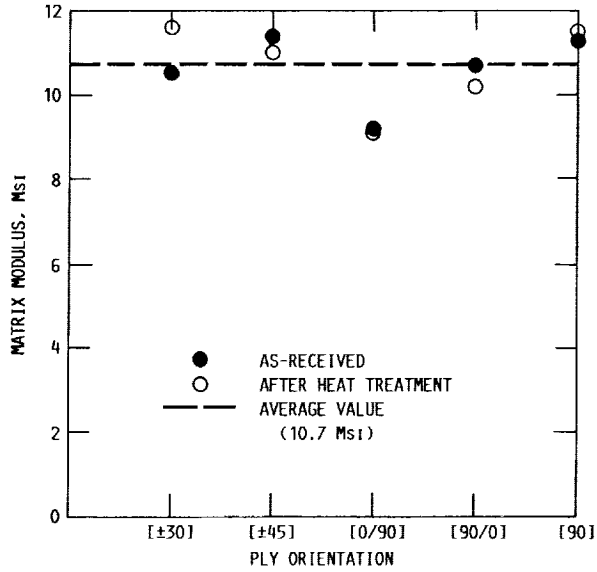

FIGURE 6. - CALCULATED MATRIX MODULUS BEFORE AND AFTER 24 HR/1292 °F HEAT TREATMENT.

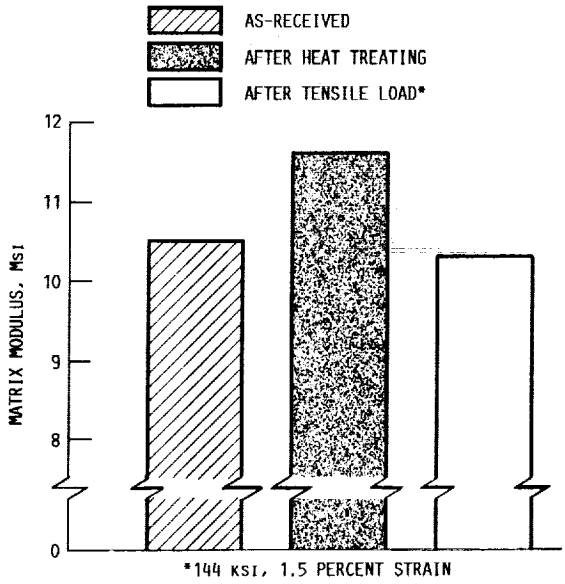

FIGURE 7. - CHANGE IN CALUCLATED MATRIX MODULUS FOR [±30] SPECIMEN DUE TO HEAT TREATMENT AND TENSILE LOAD.

NASA
National Aeronautics and Space Administration

Report Documentation Page

1. Report No.	2. Government Accession No.	3. Recipient's Catalog No.
NASA TM-102536		

4. Title and Subtitle	5. Report Date
Evaluation of Thermal and Mechanical Loading Effects on the Structural Behavior of a SiC/Titanium Composite	6. Performing Organization Code

7. Author(s)	8. Performing Organization Report No.
Joseph E. Grady and Bradley A. Lerch	E-5349
	10. Work Unit No. 505-63-11

9. Performing Organization Name and Address	11. Contract or Grant No.
National Aeronautics and Space Administration Lewis Research Center Cleveland, Ohio 44135-3191	13. Type of Report and Period Covered Technical Memorandum

12. Sponsoring Agency Name and Address	14. Sponsoring Agency Code
National Aeronautics and Space Administration Washington, D.C. 20546-0001	

15. Supplementary Notes

Prepared for the 31st Structures, Structural Dynamics and Materials Conference cosponsored by the AIAA, ASME, AHS, and ASC, Long Beach, California, April 2-4, 1990.

16. Abstract

Composite specimens of titanium-15-3 matrix reinforced with continuous SCS-6 silicon carbide fibers were tested under a variety of thermal and mechanical loadings. A combined experimental/finite element approach was used to estimate the effective in-situ modulus of the matrix material and to evaluate changes in modulus due to the applied loads. Several fiber orientations were tested. Results indicate that the effect of the thermal loads on composite stiffness varies with fiber orientation. Applications of this method to test specimens damaged by uniaxial tension, thermal cycling, and isothermal fatigue loadings are used to illustrate that by monitoring overall structural behavior, changes in stiffness caused by thermomechanical loading can be detected.

17. Key Words (Suggested by Author(s))	18. Distribution Statement
Metal matrix composites Vibration Experimental mechanics	Unclassified – Unlimited Subject Category 24

19. Security Classif. (of this report)	20. Security Classif. (of this page)	21. No. of pages	22. Price*
Unclassified	Unclassified	14	A03

*For sale by the National Technical Information Service, Springfield, Virginia 22161

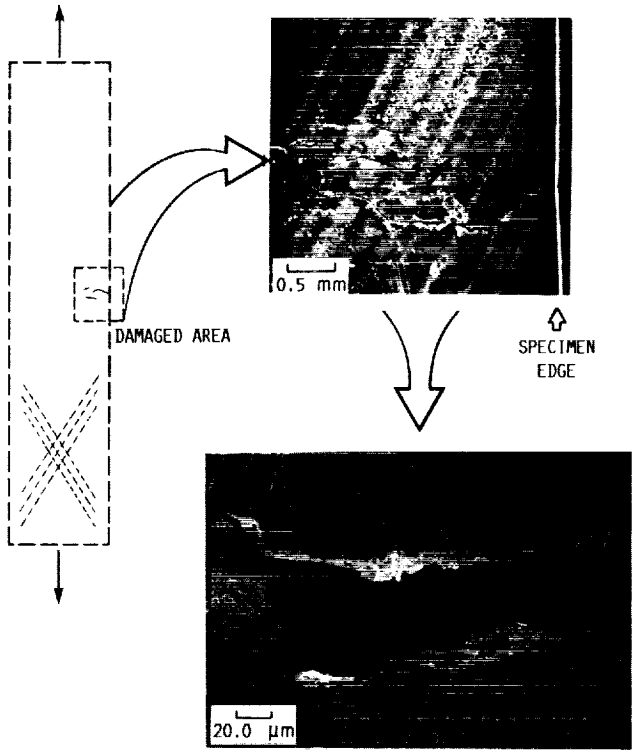

FIGURE 8. - SCANNING ELECTRON MICROSCOPE PHOTOGRAPHS OF DAMAGED AREA OF A [±30] SPECIMEN LOADED IN TENSION TO 1.5 PERCENT STRAIN.

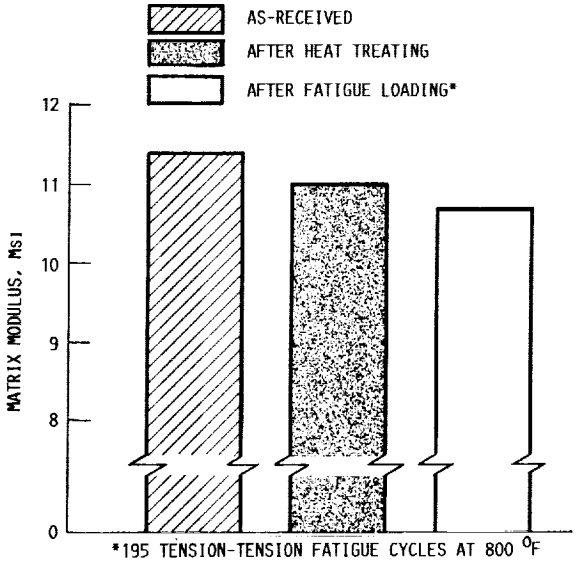

FIGURE 9. - CHANGE IN CALCULATED MATRIX MODULUS FOR [±45] SPECIMEN DUE TO HEAT TREATMENT AND FATIGUE LOAD.

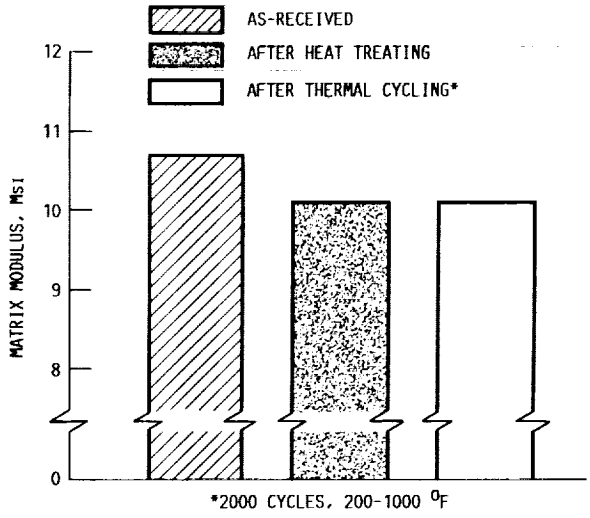

FIGURE 10. - CHANGE IN CALCULATED MATRIX MODULUS FOR [90/0] SPECIMEN DUE TO HEAT TREATMENT AND THERMAL CYCLING.